

# Kerr black hole in de Sitter spacetime and observational redshift: Toward a new method to measure the Hubble constant

Mehrab Momennia,<sup>1, a</sup> Alfredo Herrera-Aguilar,<sup>1, b</sup> and Ulises Nucamendi<sup>2, c</sup>

<sup>1</sup>*Instituto de Física, Benemérita Universidad Autónoma de Puebla,  
Apartado Postal J-48, 72570, Puebla, Puebla, Mexico*

<sup>2</sup>*Instituto de Física y Matemáticas, Universidad Michoacana de San Nicolás de Hidalgo,  
Edificio C-3, Ciudad Universitaria, CP 58040, Morelia, Michoacán, Mexico*

(Dated: May 29, 2023)

We extract the Hubble law by the frequency-shift considerations of test particles revolving the Kerr black hole in asymptotically de Sitter spacetime. To this end, we take into account massive geodesic particles circularly orbiting the Kerr-de Sitter black holes that emit redshifted photons towards a distant observer which is moving away from the emitter–black hole system. By considering this configuration, we obtain an expression for redshift in terms of the spacetime parameters, such as mass, angular momentum, and the cosmological constant. Then, we find the frequency shift of photons versus the Hubble constant with the help of some physically motivated approximations. Finally, some exact formulas for the Schwarzschild black hole mass and the Hubble constant in terms of the observational redshift of massive bodies circularly orbiting this black hole are extracted. Our results suggest a new independent general relativistic approach to obtaining the late-time Hubble constant in terms of observable quantities.

**Keywords:** Kerr black hole, de Sitter spacetime, Hubble constant, black hole rotation curves, frequency shift.

PACS numbers: 04.70.Bw, 98.80.–k, 04.40.–b, 98.62.Gq

## I. INTRODUCTION

Black holes are the densest massive objects known in nature and are among the most important and interesting solutions to the Einstein field equations. By now, they have been directly detected through gravitational waves produced by the coalescence events captured in the LIGO and Virgo observatories [1] as well as the shadow images of supermassive black holes hosted at the center of the Milky Way galaxy and the M87 galaxy revealed by the EHT Collaboration [2, 3]. Therefore, nowadays, exploring various aspects of black holes’ physics attracts much attention in the context of the general relativity theory.

Among others, inventing and developing methods to determine the black hole parameters, such as mass, charge, and angular momentum has a special place. One of the robust methods to obtain the black hole parameters was initially suggested in [4], and then developed to analytically express the mass and spin parameters of the Kerr black hole in terms of a few directly observable quantities [5]. In this general relativistic formalism, the observables are frequency shifts of photons emitted by massive geodesic particles orbiting the central black holes along with their orbital parameters.

From the theoretical point of view, the method of [4] has been applied to several black hole spacetimes, such as higher–dimensional Myers–Perry black holes [6],

Kerr–Newman black holes in de Sitter (dS) spacetime [7], the Plebanski–Demianski background [8], and spherically symmetric regular black holes [9]. In addition, the boson stars [10] as well as black holes in modified gravity [11], coupled to nonlinear electrodynamics [12], and immersed in a strong magnetic field [13] have been investigated by employing a similar procedure, i.e. finding a relation between frequency shift and compact object parameters. However, all the aforementioned attempts were based on the kinematic redshift which is not a directly measured observational quantity, unlike the total frequency shift of photons. Thus, this fact has motivated us to take into account the total redshifts of photons and obtain concise and elegant analytic formulas for the mass and spin of the Kerr black hole in terms of these directly observable elements [5]. More recently, this method was also applied to express the parameters of static polymerized black holes in terms of the total frequency shifts [14].

From a practical point of view, the developed prescription of this general relativistic approach has been employed to estimate the mass-to-distance ratio of some supermassive black holes hosted at the core of active galactic nuclei (AGNs), like NGC 4258 [15], TXS-2226-184 [16], and an additional 15 galaxies [17, 18]. These AGNs enjoy accretion disks consisting of water vapor clouds that are circularly orbiting the central supermassive black hole and emitting photons toward the distant observer, hence enabling us to estimate the mass-to-distance ratio and quantify the gravitational redshift produced by the spacetime curvature that is a general relativistic effect.

<sup>a</sup>Electronic address: mmomennia@ifuap.buap.mx, momennia1988@gmail.com

<sup>b</sup>Electronic address: aherrera@ifuap.buap.mx

<sup>c</sup>Electronic address: ulises.nucamendi@umich.mx, unucamendi@gmail.com

On the other hand, the so-called  $\Lambda$ -cold dark mat-

ter cosmological standard model successfully explains the current epoch in the evolution of the cosmos. The field equations of Einstein gravity in the presence of a cosmological constant  $\Lambda$  along with an energy-momentum tensor  $T_{\mu\nu}^m$  that accounts for the matter content of the Universe read

$$G_{\mu\nu} + \Lambda g_{\mu\nu} = T_{\mu\nu}^m, \quad (1)$$

where  $G_{\mu\nu}$  is the Einstein tensor. Thus, in order to explain the current accelerated expansion of the Universe, taking into account the contribution of the dark energy, and thus adding the  $\Lambda$ -term to the Einstein field equations is inevitable [19, 20]. Indeed, although the observations in small scales could be explained by the first term of the left-hand side (lhs) of Eq. (1), a consistent description of the large-scale structure of the Universe requires considering the second term. Therefore, it is quite natural to attempt to quantitatively clarify the influence of the repulsive cosmological constant on the detected redshift and blueshift of photons coming from massive geodesic particles, stars for instance, orbiting the Kerr black hole.

In order to advance work in this direction, we shall consider the field equations (1) in the absence of matter content as the first step. A family of solutions to these simplified field equations describes black holes in asymptotically dS spacetime. Moreover, the rotating black hole solutions to the Einstein- $\Lambda$  field equations are described by the Kerr-dS (KdS) line element [21] and the properties of the geodesic motion in this background have been investigated in [22–24] (see [7] as well). Thus, by taking into account the Universe expansion effect encoded in the cosmological constant through the explicit appearance of the  $\Lambda$  term in the metric, we push forward the formalism developed in [4, 5] for expressing the Kerr black hole parameters in terms of purely observational quantities to the case in which the Hubble constant can also be determined.

The consideration of the accelerated expansion of the Universe in the redshift due to a cosmological constant has potential interest in terms of astrophysical applications, since many of the AGNs with megamaser disks orbiting its central black hole are within the Hubble flow [25–33]. Therefore, this modeling includes the contribution of the expansion of the Universe in the metric, making it suitable for describing this effect on the total redshift of photons emitted by test particles and detected on Earth. Thus, this new form of accounting for the dS accelerated expansion of the Universe in the expression for total redshift allows us to extract the Hubble law as well. Finally, it is worth noticing that this approach differs from the previous ones in which the expansion effect is taken into account in the total redshift through a composition of redshifts that has no metric origin (see, for instance, [17, 18, 31, 33]).

The outline of this paper is as follows. The next section is devoted to a brief review of the geometrical properties of the KdS black holes and the geodesic motion

in this background. Besides, we analytically obtain the valid parameter space for having KdS black holes, and also review our general relativistic formalism that allows expressing the black hole parameters in terms of observational redshift. In Sec. III, we express the redshift of emitters that are circularly orbiting the KdS black holes in terms of the parameters of spacetime while the detector is in radial motion. Then, by considering a physically motivated configuration, we extract the Hubble law in its original formulation from the obtained frequency shift relation. Finally, we find analytic expressions for the Schwarzschild black hole mass and the Hubble constant in terms of the observational frequency shifts of photons emitted by massive particles orbiting circularly a Schwarzschild black hole. We finish our paper with some concluding remarks.

## II. KERR-DE SITTER SPACETIME

Here, we give a short review of the geometrical properties of the rotating black holes in the dS background and analytically obtain valid parameter space for having KdS black holes in Sec. II A. Then, we study the geodesic motion of massless/massive particles in this geometry in Sec. II B and derive equations that are important for our next purposes. Finally, in Sec. II C, we briefly review our general relativistic formalism that allows us to express the black hole parameters in terms of observational redshift and orbital parameters of massive geodesic particles orbiting around the black holes. We shall use the general results of this section for a special configuration in Sec. III to extract the Hubble law.

### A. Properties of the Kerr-dS background

The KdS line element in the standard Boyer-Lindquist coordinates  $(t, r, \theta, \varphi)$  reads [21] (we use  $c = 1 = G$  units)

$$ds^2 = g_{tt}dt^2 + 2g_{t\varphi}dtd\varphi + g_{\varphi\varphi}d\varphi^2 + g_{rr}dr^2 + g_{\theta\theta}d\theta^2, \quad (2)$$

with the metric components

$$g_{tt} = - \left( \frac{\Delta_r - \Delta_\theta a^2 \sin^2 \theta}{\Sigma \Xi^2} \right), \quad g_{rr} = \frac{\Sigma}{\Delta_r}, \quad g_{\theta\theta} = \frac{\Sigma}{\Delta_\theta}, \quad (3)$$

$$g_{\varphi\varphi} = \frac{\sin^2 \theta}{\Sigma \Xi^2} \left[ \Delta_\theta (r^2 + a^2)^2 - \Delta_r a^2 \sin^2 \theta \right], \quad (4)$$

$$g_{t\varphi} = - \frac{a \sin^2 \theta}{\Sigma \Xi^2} \left[ \Delta_\theta (r^2 + a^2) - \Delta_r \right], \quad (5)$$

where the functions  $\Delta_r(r)$ ,  $\Delta_\theta(\theta)$ ,  $\Sigma(r, \theta)$ , and  $\Xi$  have the following explicit form

$$\Delta_r = r^2 + a^2 - 2Mr - \frac{\Lambda r^2}{3} (r^2 + a^2), \quad (6)$$

$$\Delta_\theta = 1 + \frac{\Lambda}{3} a^2 \cos^2 \theta, \quad (7)$$

$$\Sigma = r^2 + a^2 \cos^2 \theta, \quad (8)$$

$$\Xi = 1 + \frac{\Lambda}{3} a^2, \quad (9)$$

and  $M$  is the total mass of the black hole,  $a$  is the angular momentum per unit mass  $a = J/M$ , and  $\Lambda$  is the cosmological constant related to dS radius  $l_{dS}$  as  $\Lambda = 3/l_{dS}^2$ . The KdS metric (2) describes an axially symmetric and stationary spacetime (between the event horizon and the cosmological horizon) that reduces to the standard Kerr black hole in the limit  $\Lambda = 0$  and the Schwarzschild-dS (SdS) black hole for  $a = 0$ . The coordinate singularities of this spacetime are characterized by  $\Delta_r = 0$  (the four roots correspond to horizons), while calculation of the invariant curvature scalar reveals that the intrinsic singularity is given by  $\Sigma = 0$  where located at  $\{r = 0, \theta = \pi/2\}$  for  $a \neq 0$ . Therefore, the presence of a cosmological horizon, characterized by the largest root of  $\Delta_r$ , is one of the consequences of non-vanishing  $\Lambda$ .

In order to find the extreme values of  $a$  and  $\Lambda$  for having black holes, we found that it is convenient to introduce the normalized variables  $x$ ,  $\alpha$ , and  $\lambda$  as below

$$x = \frac{r}{M}, \quad \alpha = \frac{a}{M}, \quad \lambda = \frac{\Lambda M^2}{3}, \quad (10)$$

and express the  $\Delta_r$  function in terms of the new variables as follows

$$M^{-2} \Delta_r = x^2 + \alpha^2 - 2x - \lambda x^2 (x^2 + \alpha^2). \quad (11)$$

Generally, one can show that  $\Delta_r$  has (at most) four distinct roots that can be regarded as the cosmological horizon ( $x = x_c$ ), the event horizon ( $x = x_+$ ), the inner horizon ( $x = x_-$ ), and a negative root ( $x = x_0 < 0$ ) so that  $x_- < x_+ < x_c$  (see Fig. 1). Therefore, we can express  $\Delta_r$  in terms of these quantities in the following form

$$M^{-2} \Delta_r = \lambda (x - x_0) (x - x_-) (x - x_+) (x_c - x). \quad (12)$$

Now, by equating the equations for  $\Delta_r$  given in (11) and (12), the following relations between parameters are found

$$\alpha^2 = \lambda x_- x_+ x_c (x_- + x_+ + x_c), \quad (13)$$

$$\lambda = \frac{2}{(x_- + x_+) (x_- + x_c) (x_+ + x_c)}, \quad (14)$$

$$x_0 = -(x_- + x_+ + x_c), \quad (15)$$

where  $x_-$ ,  $x_+$ , and  $x_c$  are considered as three fundamental parameters of spacetime. Similar to the Kerr

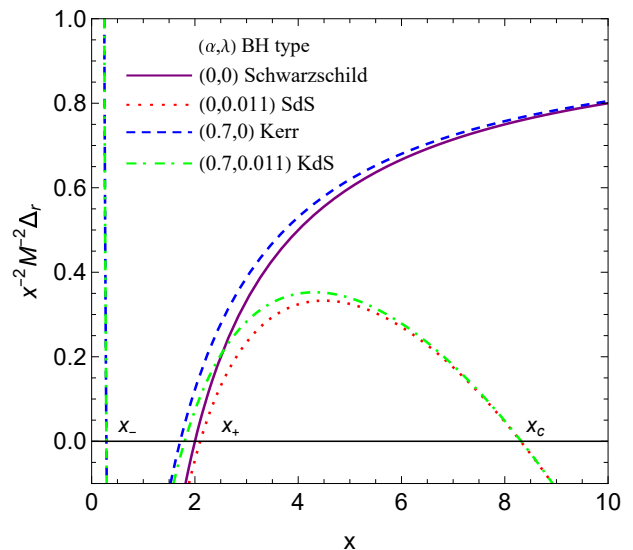


FIG. 1: The general behavior of  $\Delta_r$  function given in (11) versus the radial coordinate  $x$  for four black hole types, namely Schwarzschild, SdS, Kerr, and KdS.  $\Delta_r$  is positive between  $x_+$  and  $x_c$  as well as before  $x_-$ , whereas is negative otherwise. By increasing  $\lambda$  ( $\alpha$ ),  $x_c$  ( $x_-$ ) approaches  $x_+$  (not shown here).

case, there should be a maximum value for the rotation parameter, say  $\alpha_{\max}$ , such that we have black holes in the range  $0 \leq \alpha^2 \leq \alpha_{\max}^2$  and a naked singularity for  $\alpha^2 > \alpha_{\max}^2$ . By considering (13)-(14), and also, the condition  $x_- < x_+ < x_c$  between roots, we find that the maximum  $\alpha_{\max}$  happens whenever  $x_- \lesssim x_+ \lesssim x_c$ , hence all the horizons are closely spaced for  $\alpha_{\max}$ . Therefore, we should take into account the approximation  $x_- \approx x_+ \approx x_c$  to obtain  $\alpha_{\max}$ . On the other hand,  $0 \leq \alpha^2 \leq \alpha_{\max}^2$  and (13) show that the cosmological constant should obey the following interval as well

$$0 \leq \lambda \leq \lambda_{crit}, \quad \lambda_{crit} = \frac{\alpha_{\max}^2}{x_- x_+ x_c (x_- + x_+ + x_c)}. \quad (16)$$

Note that in order to have black holes, there is always a maximum cosmological constant, say  $\lambda_{\max}$ , which corresponds to an arbitrary rotation parameter  $\alpha$  in the range  $0 \leq \alpha \leq \alpha_{\max}$ . The maximum value of  $\lambda$ , in the general case, is corresponding to  $\alpha_{\max}$  which is denoted as critical cosmological constant  $\lambda_{crit}$  in the aforementioned inequality. Therefore, generally speaking, there is an interval for  $\lambda_{\max}$  that depends on the rotation parameter  $\alpha$ , as  $\lambda_{\max}^{(SdS)}(\alpha = 0) \leq \lambda_{\max} \leq \lambda_{crit}(\alpha = \alpha_{\max})$  so that its lower bound represents the maximum value of  $\lambda$  for the SdS black hole and  $\lambda \approx \lambda_{\max}^{(SdS)}$  characterizes the near-extremal SdS solution. In other words, there is a maximum value of  $\lambda$  for an arbitrary rotation parameter  $\alpha$ , and similarly, there is a maximum value of  $\alpha$  for an arbitrary cosmological constant  $\lambda$  (for example, for the SdS black hole with  $\alpha = 0$ , the cosmological constant ranges within  $0 \leq \lambda \leq \lambda_{\max}^{(SdS)}$ ).

Now, in order to obtain  $\alpha_{\max}$ , and then  $\lambda_{\max}^{(SdS)}$  and  $\lambda_{crit}$ , we need to take into account the condition  $x_- \lesssim x_+ \lesssim x_c$ , as we mentioned above. To do so, we first equate Eqs. (11) and (12) while considering  $x_+$  and  $x_c$  as two independent variables to obtain the following relations

$$\alpha = \sqrt{\frac{4x_+x_c + \Pi - \Upsilon}{2(x_+ + x_c)}}, \quad (17)$$

$$x_- = \frac{1}{2\sqrt{(x_c + x_+ - 2)(x_c + x_+)}} \{x_c^4 + x_+^4 + 4\Pi + 2\Upsilon + 2x_+x_c[2(x_+ + x_c + 1) - x_cx_+]\}^{\frac{1}{2}} - \frac{1}{2}(x_+ + x_c), \quad (18)$$

$$x_0 = -(x_- + x_+ + x_c), \quad (19)$$

$$\lambda = \frac{-\Pi + \Upsilon}{2x_+^2x_c^2(x_+ + x_c)}, \quad (20)$$

with  $\Pi$  and  $\Upsilon$  being

$$\Pi = \sqrt{\Upsilon^2 - 4x_+^2x_c^2(x_+ + x_c - 2)(x_+ + x_c)}, \quad (21)$$

$$\Upsilon = x_+^3 + x_+x_c(x_+ + 2) + x_c^2(x_+ + x_c). \quad (22)$$

Then, we take into account the near-extremal regime  $x_c \rightarrow x_+$  in the above-mentioned formulas, i.e. when the cosmological horizon  $x_c$  is very close to the black hole event horizon  $x_+$  ( $x_c - x_+ \ll x_+$ ). Hence, we obtain the following relations for  $\alpha$ ,  $x_-$ ,  $x_0$ , and  $\lambda$  in the nearly extreme regime

$$\alpha \approx \sqrt{\frac{x_+}{2}} \left(1 - 2x_+ + \sqrt{1 + 8x_+}\right)^{\frac{1}{2}}, \quad (23)$$

$$x_- \approx -x_+ + \sqrt{\frac{x_+}{2(x_+ - 1)}} \left(1 + 2x_+ + \sqrt{1 + 8x_+}\right)^{\frac{1}{2}}, \quad (24)$$

$$x_0 \approx -2x_+ - x_-, \quad (25)$$

$$\lambda_{\max} \approx \frac{1 + 2x_+ - \sqrt{1 + 8x_+}}{2x_+^3}, \quad (26)$$

where we replaced  $\lambda$  with  $\lambda_{\max}$  since  $x_c \approx x_+$ . Now, the maximum value of the rotation parameter,  $\alpha_{\max}$ , can be obtained by taking the limit  $x_+ \rightarrow x_-$  in the aforementioned relations. By considering  $x_- \approx x_+$  in (24), we obtain a maximum value for the event horizon as below

$$x_+ = \frac{3 + 2\sqrt{3}}{4}, \quad (27)$$

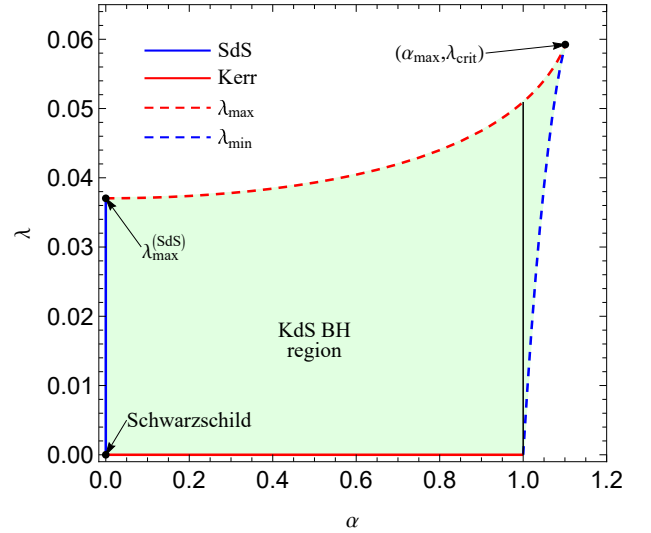


FIG. 2: The valid area of KdS black holes in  $\alpha - \lambda$  parameter space. The shaded green region belongs to KdS black holes while the marginal points on the left indicate SdS black holes and on the bottom represent standard Kerr solutions. This figure also shows how a background cosmological constant extends the parameter space.

that is indeed a coincidental point for all the three horizons ( $x_c \approx x_+ \approx x_- \approx (3 + 2\sqrt{3})/4$ ), hence it maximizes the rotation parameter in Eq. (23). Therefore, by substituting (27) in (23), we obtain

$$\alpha_{\max} = \frac{1}{4} \left(9 + 6\sqrt{3}\right)^{\frac{1}{2}} \approx 1.101, \quad (28)$$

that is slightly higher than unity for the standard Kerr black hole ( $\alpha_{\max} > \alpha_{\max}^{Kerr} = 1$ ). It is worthwhile to mention that this value corresponds to the maximum possible value of the cosmological constant,  $\lambda_{crit}$  ( $\alpha = \alpha_{\max}$ ), and therefore, it will be less for lower values of the cosmological constant. Thus, the rotation parameter ranges

$$0 \leq \alpha \leq \alpha_{\max} \quad (29)$$

with  $\alpha_{\max}$  given by (28).

Now, we obtain bounds on maximum values of the cosmological constant  $\lambda_{\max}$ , namely  $\lambda_{\max}^{(SdS)}(\alpha = 0)$  and  $\lambda_{crit}(\alpha = \alpha_{\max})$ . The maximum value for the event horizon is given in Eq. (27) that corresponds to maximally rotating black holes with  $\alpha = \alpha_{\max}$ . Therefore, by substituting Eq. (27) in Eq. (26), we obtain  $\lambda_{crit}(\alpha = \alpha_{\max}) = 16 / (3 + 2\sqrt{3})^3$ .

On the other hand, since SdS is static  $\alpha = 0$ , we set  $x_- = 0$  in (24) and obtain the maximum value of the event horizon as  $x_+ = 3 \equiv x_+^{(SdS)}$  for this case (we set  $x_- = 0$  because SdS black holes have no inner horizon). By replacing this value in Eq. (26), one can find the maximum value of the cosmological constant for the static case as  $\lambda_{\max}(\alpha = 0) = 1/27 \equiv \lambda_{\max}^{(SdS)}$ . We summarized

the results of this section on the bounds of KdS parameters as follows

$$\left\{ \begin{array}{l} 0 \leq \alpha \leq \alpha_{\max}, \\ \lambda_{\max}^{(SdS)} \leq \lambda_{\max} \leq \lambda_{crit}, \\ x_{+\max}^{(SdS)} \leq x_{+\max} \leq x_{+crit}, \end{array} \right. \quad (30)$$

with

$$\left\{ \begin{array}{l} \alpha_{\max} = \frac{1}{4} (9 + 6\sqrt{3})^{\frac{1}{2}}, \\ \lambda_{\max}^{(SdS)} = \frac{1}{27}, \quad \lambda_{crit} = \frac{16}{(3+2\sqrt{3})^3}, \\ x_{+\max}^{(SdS)} = 3, \quad x_{+crit} = \frac{3+2\sqrt{3}}{4}. \end{array} \right. \quad (31)$$

Therefore, the maximum value of the cosmological constant in the Kerr geometry must be in the aforementioned interval. For instance, the relation of  $\lambda$  given in (14) must obey  $0 \leq \lambda \leq \lambda_{\max}^{(SdS)}$  for the static case  $\alpha = 0$ , while  $\lambda = 0$  represents the standard Schwarzschild solution and  $\lambda \approx \lambda_{\max}^{(SdS)}$  denotes nearly extreme SdS black holes. Other cases far from these two extreme values and within this range are known as SdS black holes while we have a naked singularity for  $\lambda > \lambda_{\max}^{(SdS)}$ .

On the other hand, one may note that for an arbitrary value of the rotation parameter in the range  $1 < \bar{\alpha} \leq \alpha_{\max}$ ,  $\lambda$  acquires a minimum value as well and must obey  $\lambda_{\min} \leq \lambda \leq \lambda_{\max}$  for a given  $\bar{\alpha}$ . Obtaining these bounds on the parameters of KdS black holes is important since they will help us to find valid values of the redshifted photons emitted by massive particles orbiting a KdS black hole.

Various regions of KdS black holes in the  $\alpha - \lambda$  plane are illustrated in Fig. 2. In this figure, the continuous vertical blue line  $\alpha = 0$  represents SdS black holes, the continuous horizontal red line  $\lambda = 0$  shows the standard Kerr black holes, and there are standard Schwarzschild solutions where they join  $\{\alpha = 0, \lambda = 0\}$ . Extreme points  $\{\alpha = 0, \lambda = \lambda_{\max}^{(SdS)}\}$  and  $\{\alpha = \alpha_{\max}, \lambda = \lambda_{crit}\}$  that we have obtained analytically in (30) are shown on the top corners. To obtain the  $\lambda_{\max}$ -dashed line on the top of the shaded green area, we used Eqs. (23) and (26) while one can employ the relations (17)-(20) in order to find the  $\lambda_{\min}$ -dashed line on the right of the shaded green area assuming  $x_- = x_+$ . Thus, we derived all the marginal points of KdS black holes in the parameter space  $\alpha - \lambda$  *analytically* that are presented in Eqs. (17)-(20), (23)-(26), and (30). Note that some of these bounds have been found in [22] from a different approach.

It is worthwhile to mention that we have a naked singularity for  $\lambda > \lambda_{\max}$ , whereas for  $\alpha > \alpha_{\max}$ , the inner and outer horizons vanish and there is just a cosmological horizon assuming  $\lambda \neq 0$ . One can see that the non-vanishing cosmological constant introduces two important modifications to the standard Kerr geometry: (i) It

leads to a new horizon, known as the cosmological horizon, and (ii) allows having higher values for the rotation parameter. As we shall see in Sec. III A, the cosmological constant also modifies the particles' motion and leads to an upper bound on the radius of stable emitters in circular motion.

## B. Geodesics of timelike and null particles in the Kerr-dS background

The equation of motion of test massless/massive particles in the rotating spacetimes is described by the geodesic equations. In this regard, the geodesic equations can be obtained by using the separation of variables of the Hamilton-Jacobi equation. The Hamilton-Jacobi equation, for a given background  $g_{\mu\nu}(x^\rho)$ , leading to the geodesic equations can be written as [34]

$$2 \frac{\partial S}{\partial \tau} = -g^{\mu\nu} \frac{\partial S}{\partial x^\mu} \frac{\partial S}{\partial x^\nu}, \quad (32)$$

where  $S$  represents Hamilton principal function. In this relation,  $\tau$  is the proper time that parametrizes the particle worldline and is related to the affine parameter  $\sigma$  by  $\tau = \sigma m$  which  $m$  is the particle rest mass ( $\tau$  represents the affine parameter in the case of photons). For the KdS spacetime, the Hamilton principal function  $S$  can be separated as

$$S = \frac{1}{2} \eta \tau - \bar{E} t + \bar{L} \varphi + S_r(r) + S_\theta(\theta), \quad (33)$$

for both timelike ( $\eta = 1$ ) and null ( $\eta = 0$ ) particles, and  $S_r(r)$  is a function of  $r$  while  $S_\theta(\theta)$  is a function of  $\theta$  only. The constants of motion  $\bar{E}$  and  $\bar{L}$ , respectively, correspond to conserved energy  $E_0$  and angular momentum  $L_0$  of massive particles obtained through the following equations

$$\bar{E} = \frac{E_0}{m} = -g_{\mu\nu} \xi^\mu U^\nu, \quad (34)$$

$$\bar{L} = \frac{L_0}{m} = g_{\mu\nu} \psi^\mu U^\nu, \quad (35)$$

where  $\xi^\mu = \delta_t^\mu$  is the timelike Killing vector field and  $\psi^\mu = \delta_\varphi^\mu$  is the rotational Killing vector field of the spacetime, and  $U^\mu$  is the 4-velocity of particles which is normalized to unity  $U^\mu U_\mu = -1$ .

On the other hand, by substituting the decomposition (33) into the Hamilton-Jacobi equation (32), we get the

following equality

$$\begin{aligned}
& \eta a^2 \cos^2 \theta + \Delta_\theta \left( \frac{dS_\theta(\theta)}{d\theta} \right)^2 \\
& + \frac{\Xi^2}{\Delta_\theta \sin^2 \theta} (a\bar{E} \sin^2 \theta - \bar{L})^2 \\
= & -\eta r^2 - \Delta_r \left( \frac{dS_r(r)}{dr} \right)^2 \\
& + \frac{\Xi^2}{\Delta_r} [(r^2 + a^2) \bar{E} - a\bar{L}]^2, \quad (36)
\end{aligned}$$

where the lhs is a function of  $\theta$  only and the right-hand side (rhs) just depends on the  $r$ -coordinate. Therefore, either side is equal to a constant of motion, known as the Carter constant  $\mathcal{C}$  with the following form [34]

$$\mathcal{C} = \mathcal{K} + (\bar{L} - a\bar{E})^2 \Xi^2, \quad (37)$$

which  $\mathcal{K}$  is a constant that arises from the contraction of the Killing tensor field  $K_{\mu\nu}$  of Kerr-dS spacetime with the 4-velocity as  $\mathcal{K} = K_{\mu\nu} U^\mu U^\nu$ . Now, by making use of (34)–(37), and the unity condition  $U^\mu U_\mu = -1$ , we can obtain the 4-velocity components of massive particles ( $\eta = 1$ ) in terms of constants of motion  $\bar{E}$ ,  $\bar{L}$ , and  $\mathcal{K}$  as follows

$$\begin{aligned}
U^t = & \frac{\Xi^2}{\Sigma \Delta_\theta \Delta_r} \left\{ a [\Delta_r - (a^2 + r^2) \Delta_\theta] \bar{L} \right. \\
& \left. + [(a^2 + r^2)^2 \Delta_\theta - a^2 \sin^2 \theta \Delta_r] \bar{E} \right\}, \quad (38)
\end{aligned}$$

$$\begin{aligned}
\Sigma^2 (U^r)^2 = & \Xi^2 [(a^2 + r^2) \bar{E} - a\bar{L}]^2 \\
& - \Delta_r [\mathcal{K} + r^2 + \Xi^2 (\bar{L} - a\bar{E})^2] \\
\equiv & V_r(r), \quad (39)
\end{aligned}$$

$$\begin{aligned}
\Sigma^2 (U^\theta)^2 = & \Delta_\theta (\mathcal{K} - a^2 \cos^2 \theta) - a^2 \Xi^2 (\sin^2 \theta - \Delta_\theta) \bar{E}^2 \\
& - \Xi^2 \left( \frac{1}{\sin^2 \theta} - \Delta_\theta \right) \bar{L}^2 + 2a\Xi^2 (1 - \Delta_\theta) \bar{E} \bar{L} \\
\equiv & V_\theta(\theta), \quad (40)
\end{aligned}$$

$$\begin{aligned}
U^\varphi = & \frac{\Xi^2}{\Sigma \Delta_\theta \Delta_r \sin^2 \theta} \left\{ (\Delta_r - a^2 \Delta_\theta \sin^2 \theta) \bar{L} \right. \\
& \left. + a \sin^2 \theta [(a^2 + r^2) \Delta_\theta - \Delta_r] \bar{E} \right\}, \quad (41)
\end{aligned}$$

where the rhs of Eq. (39) is a function of  $r$  and the rhs of Eq. (40) is a function of  $\theta$  only. Note that Eqs. (34) and (35) have been used to obtain Eqs. (38) and (41), while Eqs. (36), (37), and the unity condition  $U^\mu U_\mu = -1$  have been employed to get the relations (39) and (40).

From Eq. (40), it is clear that the constant of motion  $\mathcal{K}$  [that is related to the Carter constant by Eq. (37)] represents a measure of how much the geodesic of particles deviates from the equatorial plane  $\theta = \pi/2$ , where this

constant vanishes. Therefore, the test particles moving in the equatorial plane have zero  $\mathcal{K}$ , whereas it is non-vanishing whenever particles cross the equatorial plane.

The first-order differential equations presented in Eqs. (38)–(41) show the geodesic equations of massive particles for every direction in the KdS background in terms of the constants of motion  $\bar{E}$ ,  $\bar{L}$ , and  $\mathcal{K}$ . These equations reduce to the corresponding relations given in [4] for Kerr geometry in the limit  $\Lambda \rightarrow 0$ , as it should be. Therefore, the cosmological constant encodes deviations of KdS black holes from the standard Kerr background.

On the other hand, a similar strategy can be followed to obtain the null geodesics of photons with 4-momentum  $k^\mu$  moving between the event horizon and cosmological horizon of the KdS spacetime. For massless test particles, the conserved energy  $\bar{E}_\gamma$  and angular momentum  $\bar{L}_\gamma$  of particles can be found through the following relations

$$\bar{E}_\gamma = -g_{\mu\nu} \xi^\mu k^\nu, \quad (42)$$

$$\bar{L}_\gamma = g_{\mu\nu} \psi^\mu k^\nu, \quad (43)$$

where the 4-momentum  $k^\mu$  of null particles satisfies  $k^\mu k_\mu = 0$ . Besides, the equality (36) takes the form

$$\begin{aligned}
& \Delta_\theta \left( \frac{dS_\theta(\theta)}{d\theta} \right)^2 + \frac{\Xi^2}{\Delta_\theta \sin^2 \theta} (a\bar{E}_\gamma \sin^2 \theta - \bar{L}_\gamma)^2 = \\
& -\Delta_r \left( \frac{dS_r(r)}{dr} \right)^2 + \frac{\Xi^2}{\Delta_r} [(r^2 + a^2) \bar{E}_\gamma - a\bar{L}_\gamma]^2, \quad (44)
\end{aligned}$$

for the null particles ( $\eta = 0$ ). Now, by making use of Eqs. (42)–(44) and  $k^\mu k_\mu = 0$ , we obtain the various components of the 4-momentum in terms of the constants of motion  $\bar{E}_\gamma$ ,  $\bar{L}_\gamma$ , and  $\mathcal{K}_\gamma$  as follows

$$\begin{aligned}
k^t = & \frac{\Xi^2}{\Sigma \Delta_\theta \Delta_r} \left\{ a [\Delta_r - (a^2 + r^2) \Delta_\theta] \bar{L}_\gamma \right. \\
& \left. + [(a^2 + r^2)^2 \Delta_\theta - a^2 \sin^2 \theta \Delta_r] \bar{E}_\gamma \right\}, \quad (45)
\end{aligned}$$

$$\begin{aligned}
\Sigma^2 (k^r)^2 = & \Xi^2 [(a^2 + r^2) \bar{E}_\gamma - a\bar{L}_\gamma]^2 \\
& - \Delta_r [\mathcal{K}_\gamma + \Xi^2 (\bar{L}_\gamma - a\bar{E}_\gamma)^2] \\
\equiv & \mathcal{V}_r(r), \quad (46)
\end{aligned}$$

$$\begin{aligned}
\Sigma^2 (k^\theta)^2 = & \Delta_\theta \mathcal{K}_\gamma - a^2 \Xi^2 (\sin^2 \theta - \Delta_\theta) \bar{E}_\gamma^2 \\
& - \Xi^2 \left( \frac{1}{\sin^2 \theta} - \Delta_\theta \right) \bar{L}_\gamma^2 + 2a\Xi^2 (1 - \Delta_\theta) \bar{E}_\gamma \bar{L}_\gamma \\
\equiv & \mathcal{V}_\theta(\theta), \quad (47)
\end{aligned}$$

$$\begin{aligned}
k^\varphi = & \frac{\Xi^2}{\Sigma \Delta_\theta \Delta_r \sin^2 \theta} \left\{ (\Delta_r - a^2 \Delta_\theta \sin^2 \theta) \bar{L}_\gamma \right. \\
& \left. + a \sin^2 \theta [(a^2 + r^2) \Delta_\theta - \Delta_r] \bar{E}_\gamma \right\}, \quad (48)
\end{aligned}$$

where the rhs of Eq. (46) is a function of  $r$ , the rhs of Eq. (47) is a function of  $\theta$ , and  $\mathcal{C}_\gamma = \mathcal{K}_\gamma + (\bar{L}_\gamma - a\bar{E}_\gamma)^2 \Xi^2$  is the corresponding Carter constant for photons.

It is worthwhile to mention that the equations given in (38)-(41) and (45)-(48), respectively, fully describe any geodesic motion of massive and massless particles in the background of KdS black holes for given sets of constants of motion  $\{\bar{E}, \bar{L}, \mathcal{K}\}$  and  $\{\bar{E}_\gamma, \bar{L}_\gamma, \mathcal{K}_\gamma\}$ . Hence, these relations govern the most general orbits of massive bodies, namely nonequatorial elliptic trajectories, and one can obtain arbitrary particular cases, such as nonequatorial circular orbits, elliptic equatorial paths, elliptic nonequatorial orbits, nonelliptic trajectories, and equatorial circular orbits by imposing some suitable boundary conditions.

### C. Frequency shift

In this section, we briefly review our previous results on the frequency shift of photons emitted by massive particles moving in an axially symmetric spacetime, a construction based on a general relativistic method [4, 5].

This formalism allows one to express the frequency shift of photons in terms of orbital parameters of radiant massive objects (stars, for instance), and the free parameters of the spacetime (the set of parameters  $\{M, a, \Lambda\}$  in our black hole case study). In this scenario, the probe particles feel the curvature of spacetime produced by the black hole and encode the properties of spacetime, characterized by black hole parameters, in the frequency shift of emitted photons. This capability allows us to estimate the black hole parameters through measuring the shift in the frequency of photons and solving an inverse problem.

The orbiting massive particles can emit electromagnetic waves towards us such that the corresponding photons travel along null geodesics from emission till detection while the information of the geometry is encoded in their frequency shift. The frequency of this photon at some position  $x_p^\mu = (x^t, x^r, x^\theta, x^\varphi)|_p$  reads

$$\omega_p = -(k_\mu U^\mu)|_p, \quad (49)$$

where the index  $p$  refers to either the point of emission  $x_e^\mu$  or detection  $x_d^\mu$  of the photon.

One can see that, in contrast to the commonly used radial velocities in Newtonian gravity which are coordinate-dependent observables,  $\omega_p$  is a general relativistic invariant quantity that keeps memory of photons from emission at  $x_e^\mu$  till detection at  $x_d^\mu$ . Therefore, in the transition from Newtonian gravity to general relativity, it is logical to take advantage of shifts in the frequency (49) rather than redshift due to changes in speed. This is because, in addition to the redshift due to speed changes, the frequency shift due to curvature of spacetime is also encoded in the observable quantity  $\omega_p$ .

The most general expression for shifts in the frequency  $\omega_p$  in axially symmetric backgrounds of the KdS form (2)

can be written as [4]

$$1 + z_{\kappa ds} = \frac{\omega_e}{\omega_d} = \frac{(E_\gamma U^t - L_\gamma U^\varphi - g_{rr} U^r k^r - g_{\theta\theta} U^\theta k^\theta)|_e}{(E_\gamma U^t - L_\gamma U^\varphi - g_{rr} U^r k^r - g_{\theta\theta} U^\theta k^\theta)|_d}, \quad (50)$$

where the 4-velocity  $U^\mu$  (of emitter/detector) and the 4-momentum  $k^\mu$  (at emitter/detector position) are given in Eqs. (38)-(41) and Eqs. (45)-(48), respectively. Hence,  $z_{\kappa ds}$  is the frequency shift that light signals emitted by massive particles orbiting a KdS black hole experience in their path along null geodesics towards a detecting observer. Since we have general forms of  $U^\mu$  and  $k^\mu$ , the KdS shift (50) includes arbitrary stable orbits, such as circular, elliptic, irregular, equatorial, nonequatorial, etc. Therefore, the frequency shifts of these photons, that are directly measured observational quantities, along with the orbital parameters of the emitter and the observer can be used to determine the black hole parameters [5].

In the rest of the paper, we shall focus on equatorial circular orbits for emitters (an important situation describing accretion disks orbiting supermassive black holes at the core of AGNs and circularly orbiting binary compact stars) and on radial motion of detectors due to the accelerated expansion of the Universe produced by the cosmological constant.

## III. FREQUENCY SHIFT IN TERMS OF BLACK HOLE PARAMETERS

In Sec. III A, we obtain the 4-velocity of emitters in equatorial circular motion in terms of the black hole parameters. Then, in Sec. III B, we express the 4-velocity of the detector in radial motion with respect to the emitter-black hole system versus the KdS parameters. We shall use these results in Sec. III C to obtain the redshift of the KdS black holes  $z_{\kappa ds}$  in terms of the parameters of spacetime for this special configuration and extract the Hubble law from some physically motivated approximations. Finally, we express the Schwarzschild mass and the Hubble constant in terms of observational redshift in Sec. III D.

### A. Emitters in circular and equatorial orbits

Usually, the accretion disks orbiting black holes can be well described by the equatorial circular motion of massive test particles around the rotating black holes and even any tilted disk should be driven to the equatorial plane of the rotating background [35]. Hence, in what follows, we concentrate our attention on the equatorial circular orbits of emitters characterized by  $\theta = \pi/2$  and  $U^r = 0 = U^\theta$ , to find the relations between KdS black hole parameters  $\{M, a, \Lambda\}$  and measured redshifts/blueshifts of light signals detected by an observer

located far away from their source. We also assume that the observer detects the photons in the equatorial plane  $\theta = \pi/2$  since accretion disks can be detected mostly in an edge-on view from Earth [26, 36], and therefore  $k^\theta = 0$  identically. With this assumption, we place the detector in the equatorial plane as well.

At this stage, we express the 4-velocity  $U^\mu$  for the equatorial circular orbits in terms of the KdS black hole parameters  $\{M, a, \Lambda\}$  in order to substitute in the frequency shift relation (50), hence find a connection between observational redshift/blueshift and KdS parameters. Therefore, by considering Eqs. (38)-(41), the non-vanishing components  $U_e^t$  and  $U_e^\varphi$  of the emitter read

$$U_e^t = \frac{a(\Delta_e - a^2 - r_e^2)L_e + [(a^2 + r_e^2)^2 - a^2\Delta_e]E_e}{r_e^2\Delta_e}\Xi, \quad (51)$$

$$U_e^\varphi = \frac{(\Delta_e - a^2)L_e + a(a^2 + r_e^2 - \Delta_e)E_e}{r_e^2\Delta_e}\Xi, \quad (52)$$

where  $L_e = \Xi\bar{L}_e$ ,  $E_e = \Xi\bar{E}_e$ ,  $\Delta_e = \Delta_r(r = r_e)$ , and  $r_e$  is the radius of the emitter. In this case, the Carter constant vanishes whereas the constants of motion  $E_e$  and  $L_e$  can be obtained by taking into account the conditions

$$V_r(r) = 0, \quad \frac{dV_r(r)}{dr} = 0, \quad (53)$$

simultaneously for having circular orbits while  $V_r(r)$  is given in Eq. (39). Therefore, one can solve these conditions to get [22]

$$E_e = \frac{r_e^{\frac{3}{2}} \left[ 1 - \frac{\Lambda}{3}(a^2 + r_e^2) \right] - 2Mr_e^{\frac{1}{2}} \pm a \left( M - \frac{\Lambda r_e^3}{3} \right)^{\frac{1}{2}}}{r_e^{\frac{3}{4}} \sqrt{r_e^{\frac{3}{2}} \left( 1 - \frac{\Lambda a^2}{3} \right) - 3Mr_e^{\frac{1}{2}} \pm 2a \left( M - \frac{\Lambda r_e^3}{3} \right)^{\frac{1}{2}}}}, \quad (54)$$

$$L_e = \frac{(a^2 + r_e^2) \left[ \pm \left( M - \frac{\Lambda r_e^3}{3} \right)^{\frac{1}{2}} - \frac{a\Lambda}{3} r_e^{\frac{3}{2}} \right] - 2aMr_e^{\frac{1}{2}}}{r_e^{\frac{3}{4}} \sqrt{r_e^{\frac{3}{2}} \left( 1 - \frac{\Lambda a^2}{3} \right) - 3Mr_e^{\frac{1}{2}} \pm 2a \left( M - \frac{\Lambda r_e^3}{3} \right)^{\frac{1}{2}}}}, \quad (55)$$

in terms of the KdS black hole parameters while the upper sign corresponds to a co-rotating object and the lower sign refers to a counter-rotating object with respect to the angular velocity of the black hole, and we shall use this convention in the upcoming equations.

Now, by substituting relations (54) and (55) into Eqs. (51) and (52), we can obtain rather simple equations as follows

$$U_e^t(r_e, \pi/2) = \frac{r_e^{\frac{3}{2}} \pm a \left( M - \frac{\Lambda r_e^3}{3} \right)^{\frac{1}{2}}}{\mathcal{X}_\pm} \Xi, \quad (56)$$

$$U_e^\varphi(r_e, \pi/2) = \pm \frac{\left( M - \frac{\Lambda r_e^3}{3} \right)^{\frac{1}{2}}}{\mathcal{X}_\pm} \Xi, \quad (57)$$

with

$$\mathcal{X}_\pm = r_e^{\frac{3}{4}} \sqrt{r_e^{\frac{3}{2}} \left( 1 - \frac{\Lambda a^2}{3} \right) - 3Mr_e^{\frac{1}{2}} \pm 2a \left( M - \frac{\Lambda r_e^3}{3} \right)^{\frac{1}{2}}}. \quad (58)$$

From Eqs. (56)-(58), it is obvious that one should follow the conditions  $3M - \Lambda r_e^3 \geq 0$  and  $\mathcal{X}_\pm^2 > 0$  in order to have the equatorial circular orbits. The former puts an upper bound on the emitter radius as  $r_e^3 \leq 3M/\Lambda$ , a quantity that must be located within the cosmological horizon. We call this special distance  $\bar{r} = (3M/\Lambda)^{1/3}$  as *zero gravity radius* (ZGR), a radius where the effective gravity vanishes, as we shall show below. With the quantities given in (56)-(58) at hand, we can also obtain the angular velocity of an emitter orbiting around the KdS black hole in a circular and equatorial orbit as below

$$\Omega_\pm = \frac{U_e^\varphi}{U_e^t} = \pm \frac{\left( M - \frac{\Lambda r_e^3}{3} \right)^{\frac{1}{2}}}{r_e^{\frac{3}{2}} \pm a \left( M - \frac{\Lambda r_e^3}{3} \right)^{\frac{1}{2}}}. \quad (59)$$

Besides, the non-vanishing components of the 4-momentum of photons  $k^\mu$ , given in equations (45)-(48), in the equatorial plane reduce to

$$k^t = \frac{a(\Delta_r - a^2 - r^2)L_\gamma + [(a^2 + r^2)^2 - a^2\Delta_r]E_\gamma}{r^2\Delta_r}\Xi, \quad (60)$$

$$r^2(k^r)^2 = [(a^2 + r^2)E_\gamma - aL_\gamma]^2 - \Delta_r(L_\gamma - aE_\gamma)^2, \quad (61)$$

$$k^\varphi = \frac{(\Delta_r - a^2)L_\gamma + a(a^2 + r^2 - \Delta_r)E_\gamma}{r^2\Delta_r}\Xi, \quad (62)$$

with  $L_\gamma = \Xi\bar{L}_\gamma$  and  $E_\gamma = \Xi\bar{E}_\gamma$ .

On the other hand, the condition for having stable orbits in KdS geometry is given by

$$V_r'' \equiv \frac{d^2V_r(r)}{dr^2} = -[r^2 + (L - aE)^2] \Delta_r'' - 4r\Delta_r' - 2\Delta_r + 4(3r^2 + a^2)E^2 - 4aLE \leq 0, \quad (63)$$

where prime denotes  $\partial_r$  and one can use either upper/lower sign of Eqs. (54) and (55) to obtain radii of stable circular orbits of co/counter-rotating stars. However, the polynomial expression (63) is of 10th-order in  $r$  and could not be solved analytically, unlike the standard Kerr case.

The general behavior of  $V_r''$  is illustrated through Fig. 3 for various values of  $\Lambda$  and  $a$  as well as co/counter-rotating classes. As one can see from this figure, the roots of relation (63) characterize the innermost stable circular orbit (ISCO)  $r_{ISCO}$  and outermost stable circular orbit (OSCO)  $r_{OSCO}$  describing, respectively, the inner edge of orbiting accretion disk and its outer edge. Therefore, we expect that the lower constraint on the



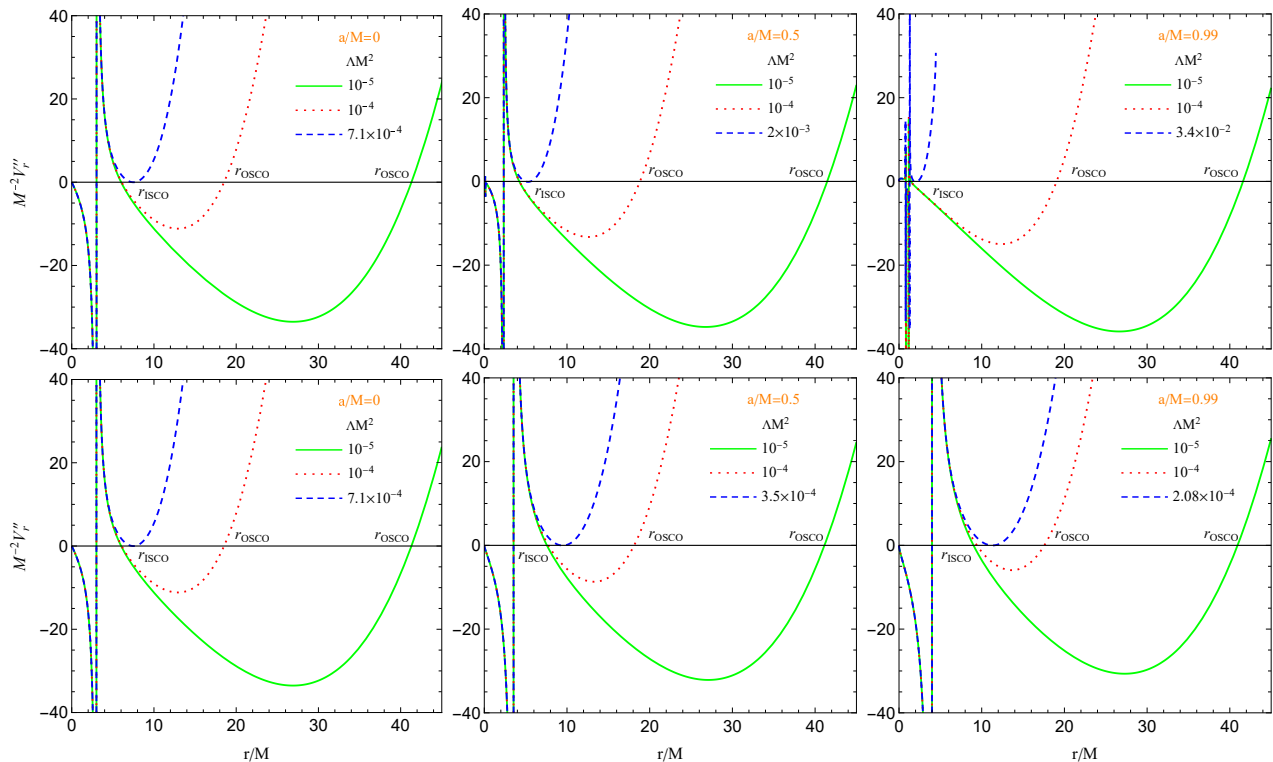


FIG. 3: The general behavior of  $V_r''$  versus the radial coordinate for the co-rotating branch (upper panels) and counter-rotating branch (lower panels).  $V_r''$  is negative between  $r_{ISCO}$  and  $r_{OSCO}$ , indicating a stable orbit area.  $r_{OSCO}$  approaches  $r_{ISCO}$  as the cosmological constant increases, and finally, there will be no stable equatorial circular orbits for sufficiently large  $\Lambda$ .

emitter radius as  $r_e \geq r_{ISCO}$  leads to an upper bound on the redshift/blueshift of orbiting objects, whereas the upper constraint  $r_e \leq r_{OSCO}$  puts a lower bound on the frequency shift.

Now, it is worthwhile to summarize the most important radii in the KdS geometry as follows

$$r_0 < 0 < r_- < r_+ < r_{ISCO} < r_{OSCO} < \bar{r} < r_c, \quad (64)$$

where (i) the inner horizon  $r_-$ , the event horizon  $r_+$ , and the cosmological horizon  $r_c$  are the solutions of  $\Delta_r$  in Eq. (6), (ii)  $r_{ISCO}$  and  $r_{OSCO}$  are the solutions of the stability condition in Eq. (63), and (iii) the ZGR  $\bar{r} = (3M/\Lambda)^{1/3}$  is a maximum radius for having the equatorial circular orbits obtained through (56)-(58).

In this study, we are interested in stable orbits satisfying  $r_{ISCO} \leq r_e \leq r_{OSCO}$  for the emitter and far away detectors with the condition

$$\bar{r} < r_d < r_c, \quad (65)$$

describing black hole systems in the Hubble flow. However, note that some of the important radii (64) may change/vanish under certain circumstances, as we discussed in Sec. II A (for  $r_-$ ,  $r_+$ , and  $r_c$ ) and in Fig. 3 (for  $r_{ISCO}$  and  $r_{OSCO}$ ). In addition, we restrict our calculations to  $\Lambda \leq 10^{-4}$  in order to have stable orbits, in consistency with Fig. 3.

## B. Detectors in radial motion

Here, we should note that the situation for the KdS geometry differs from the previous cases studied before (see [4, 5, 9, 11] and references therein) and we cannot consider circular orbiting or static detectors since the behavior of  $z_{KdS}$  in Eq. (50) versus  $\Lambda$  turns out to be unphysical once we take into account the circular orbits beyond  $\bar{r}$ . Indeed, because of the accelerated expansion of the Universe due to the positive cosmological constant at large scales, the detector should move away from the black hole in the case of far-away detectors that we are interested in. Therefore, in this case, we consider a detector that radially moves away from the KdS black hole instead of usual circularly orbiting or static detectors. This implies that  $U_d^\varphi = 0 = U_d^\theta$ , hence the non-vanishing components of the 4-velocity of the detector read [see Eqs. (38)-(41)]

$$U_d^t = \frac{(a^2 + r_d^2)^2 - a^2 \Delta_d}{r_d^2 \Delta_d} E_d \Xi, \quad (66)$$

$$(U_d^r)^2 = \frac{(a^2 + r_d^2)^2 E_d^2 - \Delta_d (r_d^2 + a^2 E_d^2)}{r_d^4}, \quad (67)$$

where we have set  $L_d = 0$  due to the radial motion of the detector,  $E_d = \Xi \bar{E}_d$ ,  $\Delta_d = \Delta_r(r = r_d)$ , and  $r_d$  is the distance between the black hole and the detector.

Note that  $U_d^\varphi = 0$  is just valid for far enough detectors, otherwise the rotation nature of the spacetime drags the detector, as it can be seen from Eq. (41).

As the next step, we need to obtain  $E_d$  in terms of the parameters of the spacetime  $\{M, a, \Lambda\}$ . One may note that at some radius  $r_d = R$ , where the gravitational attraction generated by the black hole mass is completely balanced by the expansion of the Universe produced by the cosmological constant, such that  $M = M_\Lambda$ , with  $M_\Lambda$  being an effective mass related to the cosmological constant. Thus, the radial velocity  $U_d^r$  (67) vanishes at  $r_d = R$  because the repulsive nature of the cosmological constant is exactly cancelled by the gravitational attraction. We obtain the effective mass  $M_\Lambda$  through the following integral

$$M_\Lambda = \int_0^R 4\pi\rho_\Lambda r^2 dr, \quad (68)$$

where the density of cosmological constant  $\rho_\Lambda$  is related to the cosmological constant via  $\rho_\Lambda = \Lambda/(8\pi G)$  [20]. By performing this integral and equating  $M = M_\Lambda$ , we find the vanishing velocity radius as  $R = (3M/\Lambda)^{1/3}$  that is exactly equal to the ZGR  $\bar{r}$ . Therefore, this is the radius at which the cosmological constant compensates the gravitational attraction of the black hole, and hence the effective gravity vanishes as we discussed after Eq. (58). Note that the angular velocity of the emitter (57) also vanishes for  $r_e = (3M/\Lambda)^{1/3}$  which means the emitter is static at this point as well.

Now, by replacing  $r_d = R = (3M/\Lambda)^{1/3}$  in Eq. (67) and solving  $U_d^r(r_d = R) = 0$ , one can find the energy of the detector as below

$$E_d = \left( \frac{3a^2 \left[ \left(\frac{3M}{\Lambda}\right)^{1/3} - M \right] - 9M \left[ \left(\frac{3M}{\Lambda}\right)^{2/3} - \frac{1}{\Lambda} \right]}{a^2 \left(\frac{3M}{\Lambda}\right)^{1/3} (3 + \Lambda a^2) + 9M \left(a^2 + \frac{1}{\Lambda}\right)} \right)^{\frac{1}{2}}. \quad (69)$$

In this way, the 4-velocity components (66)-(67) can be written as

$$U_d^t = \left( \frac{3a^2 \left[ \left(\frac{3M}{\Lambda}\right)^{1/3} - M \right] - 9M \left[ \left(\frac{3M}{\Lambda}\right)^{2/3} - \frac{1}{\Lambda} \right]}{a^2 \left(\frac{3M}{\Lambda}\right)^{1/3} (3 + \Lambda a^2) + 9M \left(a^2 + \frac{1}{\Lambda}\right)} \right)^{\frac{1}{2}} \times \frac{(a^2 + r_d^2)^2 - a^2 \Delta_d}{r_d^2 \Delta_d} \Xi, \quad (70)$$

$$(U_d^r)^2 = \left( \frac{3a^2 \left[ \left(\frac{3M}{\Lambda}\right)^{1/3} - M \right] - 9M \left[ \left(\frac{3M}{\Lambda}\right)^{2/3} - \frac{1}{\Lambda} \right]}{a^2 \left(\frac{3M}{\Lambda}\right)^{1/3} (3 + \Lambda a^2) + 9M \left(a^2 + \frac{1}{\Lambda}\right)} \right) \times \frac{(a^2 + r_d^2)^2 - \Delta_d a^2}{r_d^4} - \frac{\Delta_d}{r_d^2}, \quad (71)$$

in terms of the black hole parameters.

### C. Frequency shift versus parameters of spacetime and the Hubble law

For this configuration, i.e. circularly orbiting emitters and radial motion of detectors, the general expression for the frequency shift of photons (50) reduces to

$$1 + z_{\text{KdS}1,2} = \frac{(E_\gamma U^t - L_\gamma U^\varphi)|_e}{(E_\gamma U^t - g_{rr} U^r k^r)|_d} = \frac{U_e^t - b_{e(\mp)} U_e^\varphi}{U_d^t - g_d U_d^r \left(\frac{k_d^r}{E_\gamma}\right)}, \quad (72)$$

where we defined the light bending parameter  $b$  as  $b \equiv L_\gamma/E_\gamma$  that represents the deflection of light due to gravitational field in the vicinity of the KdS black hole. Besides,  $g_d = g_{rr}(r = r_d)$  is given in (3) and the ratio  $k_d^r/E_\gamma$  can be written as (from Eq. (61))

$$\left(\frac{k_d^r}{E_\gamma}\right)^2 = \frac{[(a^2 + r_d^2) - ab_{d(\mp)}]^2 - \Delta_d (b_{d(\mp)} - a)^2}{r_d^2}. \quad (73)$$

Note that  $b$ , presented in Eqs. (72) and (73), is preserved along the whole light path followed by photons from their emission till their detection due to the fact that  $E_\gamma$  and  $L_\gamma$  are constants of motion. Therefore, one can set  $b_e = b_d$  without loss of generality. Moreover, the subscript  $(\mp)$  signs refer to the deflection of light  $b$  at either side of the line of sight, whereas the subindices  $_1$  and  $_2$  in Eq. (72) correspond to the  $(-)$  and  $(+)$  signs, respectively.

On the other hand, the maximum value of the light bending parameter is given by the condition  $k^r = 0$ , where the position vector of orbiting stars with respect to the black hole center is approximately orthogonal to the line of sight. Thus, we substitute  $k^t$  and  $k^\varphi$  from Eqs. (42)-(43) as well as the condition  $k^r = 0$  in the photons' equation of motion

$$k^\mu k_\mu = 0 = g_{tt} k^t k^t + g_{rr} k^r k^r + g_{\varphi\varphi} k^\varphi k^\varphi + 2g_{t\varphi} k^t k^\varphi, \quad (74)$$

to find the maximum value of the light bending parameter for the rotating metric (2) as follows

$$b_{(\pm)} = -\frac{g_{t\varphi}(\pm) \sqrt{g_{t\varphi}^2 - g_{tt} g_{\varphi\varphi}}}{g_{tt}}, \quad (75)$$

where in terms of the KdS black hole parameters, we have

$$b_{(\pm)} = \frac{1}{r \left[1 - \frac{\Lambda}{3}(r^2 + a^2)\right] - 2M} \times \left[ -2Ma - \frac{\Lambda}{3} ar (r^2 + a^2) \right. \\ \left. (\pm) r \sqrt{r^2 + a^2 - 2Mr - \frac{\Lambda r^2}{3}(r^2 + a^2)} \right] \quad (76)$$

for equatorial circular orbits. In this formula, the sign of  $b$  denotes the redshifted and blueshifted photons when their source is co-rotating with respect to the black

hole angular momentum, and vice versa if it is counter-rotating. In other words, in the frequency shift formulas [like Eq. (72)], the minus sign enclosed in parentheses corresponds to the redshifted photons, whereas the plus sign indicates blueshifted ones.

Now, we can substitute  $g_d$ ,  $U_e^t$ ,  $U_e^\varphi$ ,  $U_d^t$ ,  $U_d^r$ ,  $k_d^r/E_\gamma$ , and  $b_{e(\mp)}$ , respectively, from Eqs. (3), (56), (57), (70), (71), (73), and (76) into (72) to find the final expressions for the redshift  $z_{KdS_1}$  and blueshift  $z_{KdS_2}$  of the KdS spacetime as follows

$$1 + z_{KdS_1} = \frac{r_e^{\frac{3}{2}} \pm a \left( M - \frac{\Lambda r_e^3}{3} \right)^{\frac{1}{2}} \pm b_{e_-} \left( M - \frac{\Lambda r_e^3}{3} \right)^{\frac{1}{2}}}{\Gamma \mathcal{X}_\pm}, \quad (77)$$

$$1 + z_{KdS_2} = 1 + z_{KdS_1} \{ b_{e_-} \rightarrow b_{e_+} \}, \quad (78)$$

with

$$\Gamma = \frac{1}{r_d^2 \Delta_d \Xi} \left\{ \left[ (a^2 + r_d^2)^2 - a^2 \Delta_d \right] E_d \Xi - \sqrt{(a^2 + r_d^2)^2 E_d^2 - \Delta_d (r_d^2 + a^2 E_d^2)} \times \sqrt{[(a^2 + r_d^2) - a b_{e_-}]^2 - \Delta_d (b_{e_-} - a)^2} \right\}, \quad (79)$$

where  $b_{e_-} = b_{(-)}|_{r=r_e}$ ,  $b_{e_+} = b_{(+)}|_{r=r_e}$ , and the upper (lower) sign refers to a co- (counter-) rotating emitter. Note that the explicit expressions of  $z_{KdS_{1,2}}$  in terms of the black hole parameters have cumbersome forms, but are not hard to be found since it is a matter of substituting  $\mathcal{X}_\pm$ ,  $\Delta_d$ ,  $\Xi$ ,  $b_{e_-}$ , and  $E_d$  in the above-mentioned equations.

The general behavior of  $z_{KdS_{1,2}}$  versus the detector radius  $r_d$  for different values of the cosmological constant is illustrated in Fig. 4. Interestingly, one can see that the shift in frequency of photons increases as the cosmological constant  $\Lambda$  increases. On the other hand, the farther the detector is from the source, the higher shift in frequency it observes. This is because the amount of dark energy between the emitter and detector increases by increasing the distance leading to larger changes in the frequency. This is what we expected from the repulsive nature of the cosmological constant, and in this study, the change in the frequency shift due to this effect is quantified through Eqs. (77)-(78). This fact leads one to extract the Hubble law in its original form from  $z_{KdS_{1,2}}$  by taking into account some physically motivated approximations as we shall show below.

Before deriving the Hubble law, one may note that the frequency shift of KdS black holes (72) contains two components including the gravitational redshift  $z_g$  as well as kinematic redshifts and blueshifts  $z_{kin_\pm}$  so that (see [5] for more details)

$$z_{KdS_{1,2}} = z_g + z_{kin_\pm}. \quad (80)$$

The gravitational redshift  $z_g$  of circular motion in the equatorial plane around the KdS background reads

$$z_g = \frac{U_e^t - b_c U_e^\varphi}{U_d^t - g_d U_d^r \left( \frac{k_d^r}{E_\gamma} \right)}, \quad (81)$$

where  $b_c$  is the light bending parameter of a light ray emitted radially at the central point (on the line of sight). The central light bending  $b_c$  is a non-vanishing quantity in rotating spacetimes due to the dragging effect and can be obtained by considering the condition  $k^\varphi$  as follows

$$b_c = -\frac{g_{t\varphi}}{g_{tt}} = -\frac{6M + \Lambda r_e (r_e^2 + a^2)}{3r_e - 6M - \Lambda r_e (r_e^2 + a^2)} a, \quad (82)$$

where the second equality refers to the equatorial circular orbits around the KdS black hole. Having the gravitational redshift  $z_g$  (81) and the central light bending parameter  $b_c$  (82) at hand, we are able to quantify all three frequency shift components, namely the KdS shift  $z_{KdS_{1,2}}$ , the gravitational redshift  $z_g$ , and the kinematic redshift  $z_{kin_\pm}$  by considering the relation (80) (note that  $b_{d(\mp)}$  in Eq. (73) should also be modified to  $b_c$ ). The importance of these relations becomes more clear when one is going to quantify the contribution of the gravitational redshift in the vicinity of a compact object. However, in what follows, we concentrate our attention on the KdS frequency shift  $z_{KdS_{1,2}}$  which is an observable quantity.

It is worth mentioning that for real astrophysical systems consisting of supermassive black holes orbited by an accretion disk containing photon sources in the form of water vapor clouds (the so-called megamasers), usually, the emitter radius is at sub-parsec scale ( $r_e < 1pc$ ) while the detector radius is at tens of mega-parsec scale to be within the Hubble flow ( $r_d > 30Mpc$ ). On the other hand, the mass and angular momentum of the black holes are of the event horizon radius order  $M, a \sim r_+$ , and the cosmological constant is of the order  $\Lambda \sim 10^{-52} m^{-2}$  [20]. Therefore, for a configuration including a supermassive black hole of the order of  $10^6$  solar masses in the Hubble flow, we have  $r_+ \sim 10^{10} m$ ,  $r_e < 10^6 r_+$ ,  $r_d > 10^{13} r_+$ , and  $\Lambda \sim 10^{-32} r_+^{-2}$  which leads to the following facts

$$\Lambda a^2 \sim 10^{-32}; \quad \Lambda r_e^2 < 10^{-20}; \quad \frac{M}{r_d} < 10^{-13}, \quad (83)$$

$$\frac{M}{r_e} > 10^{-6}; \quad \Lambda r_d^2 > 10^{-6}. \quad (84)$$

Hence, we can ignore the negligible terms  $\{\Lambda a^2, \Lambda r_e^2, M/r_d\}$  and keep dominant terms  $\{M/r_e, \Lambda r_d^2\}$  for tracking the general relativistic effects. As the next stage, we expand Eqs. (77)-(78) for  $\{\Lambda r_e^2 \rightarrow 0, \Lambda a^2 \rightarrow 0, M/r_d \rightarrow 0, \Lambda r_d^2 \rightarrow 0\}$  and keep the first dominant term in  $\Lambda r_d^2$ , to get

$$1 + z_{KdS_{1,2}} \approx \left( 1 + z_{Kerr_{1,2}} \right) (1 + z_\Lambda), \quad (85)$$

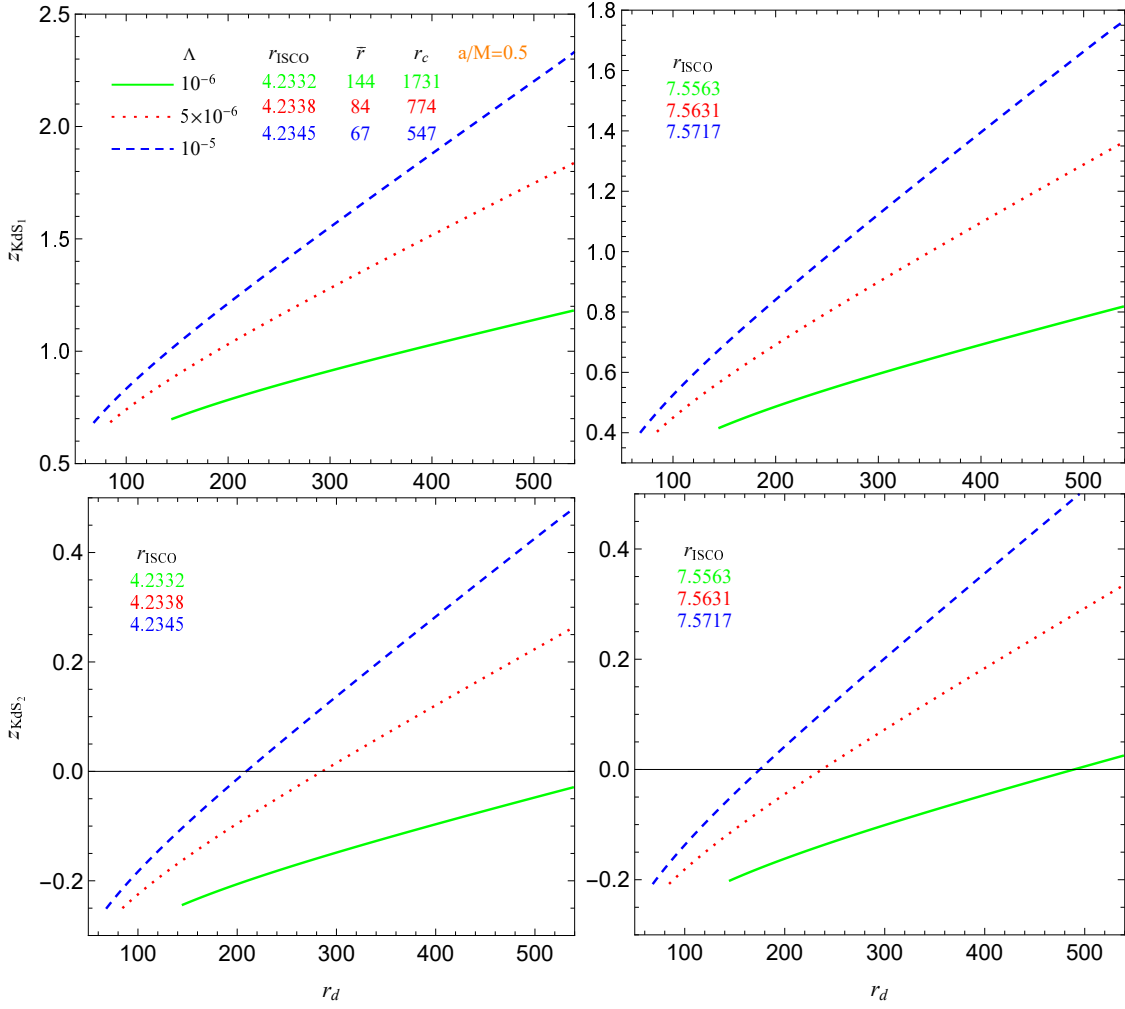


FIG. 4: The redshift  $z_{KdS_1}$  and blueshift  $z_{KdS_2}$  versus the detector distance  $r_d$  for the co-rotating branch (left panels) and counter-rotating branch (right panels). The emitter is orbiting circularly at the radius  $r_e = 2r_{\text{ISCO}}$  for either curve, and we set  $M = 1$ . The curves start at ZGR  $r_d = \bar{r} = (3M/\Lambda)^{1/3}$  on the left and terminate before the cosmological horizon  $r_d < r_c$  on the right.

where  $z_\Lambda = \sqrt{\Lambda/3}r_d$  is the contribution of the cosmological constant in the redshift, and the factors  $1 + z_{Kerr_{1,2}}$  have the following explicit forms

$$1 + z_{Kerr_1} = \frac{(1 - 2\tilde{M}) \pm \tilde{M}^{1/2} (\tilde{a} + \sqrt{\tilde{\Delta}_{Kerr}})}{(1 - 2\tilde{M}) \sqrt{1 - 3\tilde{M} \pm 2\tilde{a}\tilde{M}^{1/2}}}, \quad (86)$$

$$1 + z_{Kerr_2} = \frac{(1 - 2\tilde{M}) \pm \tilde{M}^{1/2} (\tilde{a} - \sqrt{\tilde{\Delta}_{Kerr}})}{(1 - 2\tilde{M}) \sqrt{1 - 3\tilde{M} \pm 2\tilde{a}\tilde{M}^{1/2}}}, \quad (87)$$

that are the frequency shifts in the standard Kerr space-time found in [5] with  $\tilde{M} = M/r_e$ ,  $\tilde{a} = a/r_e$ , and  $\tilde{\Delta}_{Kerr} = 1 + \tilde{a}^2 - 2\tilde{M}$ .

The Hubble constant  $H_0$  is related to the cosmological

constant with [20]

$$H_0 = \sqrt{\frac{\Lambda}{3\Omega_\Lambda}}, \quad (88)$$

where  $\Omega_\Lambda$  is the cosmological constant density parameter. For the special case of  $\Omega_\Lambda = 1$  (the Universe filled with dark energy, i.e. in the absence of matter), we recover the Hubble law from  $z_\Lambda = \sqrt{\Lambda/3}r_d$  as

$$z_\Lambda = H_0 r_d, \quad (89)$$

in which  $z_\Lambda$  represents the velocity of the host galaxy going away from the detector and  $r_d$  is the distance between the black hole and the observer. By introducing the relation (88) in Eq. (85), we can obtain the frequency shift in the KdS background in terms of the Kerr black hole parameters and the Hubble constant as below

$$1 + z_{KdS_{1,2}} \approx (1 + z_{Kerr_{1,2}}) (1 + \sqrt{\Omega_\Lambda} H_0 r_d), \quad (90)$$

an expression that can be employed to obtain  $H_0$  as well as black hole parameters. Therefore, we extracted the Hubble law by considering the frequency shift of stars orbiting around Kerr black holes in asymptotically dS spacetime detected by a far-away observer.

Note that the formula (90) does not constitute a simple multiplication of  $1 + z_{Kerr1,2}$  and  $1 + \sqrt{\Omega_\Lambda} H_0 r_d$  by hand, since here the second factor arose quite naturally as a dominant term of the cosmological redshift from general relativistic considerations, while the most general and complicated expressions are given through the rhs of Eqs. (77)-(78). This formula suggests that the photons emitted from massive geodesic particles revolving KdS black hole contain information about mass  $M$ , spin  $a$ , and the cosmological constant  $\Lambda$  when they arrive at the detector. This information is encoded in the frequency shift of these photons, denoted by  $z_{KdS1,2}$  in Eq. (90), and is a directly observable quantity. Hence, the set of spacetime parameters  $\{M, a, \Lambda\}$  can be estimated by performing a statistical fit [15–18] and sometimes analytically expressed by solving an inverse problem like in [5]. In other words, the formula (90) allows extracting the properties of spacetime characterized by the black hole mass  $M$  and spin  $a$  as well as the cosmological constant  $\Lambda$  through measuring shifts in the frequency of photons  $z_{KdS1,2}$ .

#### D. Schwarzschild black hole mass and the Hubble constant in terms of redshift/blueshift

Here, we obtain analytical formulas for the Schwarzschild black hole mass and the Hubble constant in terms of frequency shifts of photons. Then, we recover the Hubble law from the latter analytic expression.

For the static Schwarzschild black holes, the redshift formula (90) reduces to (for  $\Omega_\Lambda = 1$ )

$$1 + z_{SdS1,2} \approx \left(1 + z_{Schw1,2}\right) (1 + H_0 r_d), \quad (91)$$

where  $z_{SdS1,2}$  is the frequency shift of SdS black holes and  $z_{Schw1,2}$  is the frequency shift of the Schwarzschild black holes that can be determined by taking the limit  $\tilde{a} \rightarrow 0$  in (86)-(87) as follows

$$1 + z_{Schw1,2} = \frac{1}{\sqrt{1 - 3\tilde{M}}} \left(1 \pm \sqrt{\frac{\tilde{M}}{1 - 2\tilde{M}}}\right), \quad (92)$$

in which the upper (lower) sign refers to redshifted (blueshifted) particles [37]. Now, one can use Eqs. (91) and (92) to get

$$RB = \frac{(1 + H_0 r_d)^2}{1 - 2\tilde{M}}, \quad (93)$$

$$\frac{R}{B} = \frac{1 - \tilde{M} + 2\sqrt{\tilde{M}(1 - 2\tilde{M})}}{1 - 3\tilde{M}}, \quad (94)$$

where  $R = 1 + z_{SdS1}$  and  $B = 1 + z_{SdS2}$ . As the next step, we solve the first equation (93) to obtain the Schwarzschild black hole mass as below

$$\tilde{M} = \frac{RB - (1 + H_0 r_d)^2}{2RB}, \quad (95)$$

in terms of the frequency shift and  $H_0 r_d$  product. It is worth noticing that when the  $H_0$  constant vanishes, we recover the mass formula as a function of  $R$  and  $B$  obtained in [5]. In order to find the dependency of  $H_0 r_d$ -term on the redshift, we replace (95) in Eq. (94) and solve for  $H_0$  as

$$H_0 = \frac{1}{r_d} \left(-1 + \frac{(R + B)\sqrt{RB}}{\sqrt{3R^2 + 3B^2 - 2RB}}\right), \quad (96)$$

which gives the Hubble constant in terms of the frequency shift  $R$  and  $B$  of the massive geodesic particles on either side of the Schwarzschild black hole as well as the detector distance to the black hole  $r_d$ . Therefore, the  $H_0 r_d$  product appearing in (96) can be used to express the mass relation (95) in terms of the redshift and blueshift only. Alternatively, from Eq. (94) it is straightforward to obtain the following expression

$$\tilde{M} = \frac{(R - B)^2}{3R^2 + 3B^2 - 2RB}, \quad (97)$$

for the mass parameter defined by purely observational quantities  $R$  and  $B$ .

For the special case  $\tilde{M} \ll 1$ , we obtain  $R \approx B$  (see Eq. (94)). In this situation, the redshift  $z_{SdS1}$  and blueshift  $z_{SdS2}$  are almost equal  $z_{SdS1} \approx z_{SdS2} \equiv z$ . Thus, we recover the Hubble law for this case from the analytic expression (96) by taking the limit  $R \rightarrow B$  as follows

$$z = H_0 r_d. \quad (98)$$

It is worthwhile to mention that finding a relation of the form (91) [or Eq. (90) for the rotating case] has another significant importance practically. For instance, in the case of accretion disks circularly orbiting supermassive black holes in the center of AGNs within the Hubble flow, the total redshift of emitted photons is given by

$$1 + z_{tot1,2} = \left(1 + z_{Schw1,2}\right) (1 + z_{rec}), \quad (99)$$

in which the recessional redshift of galaxies  $z_{rec}$  is composed by [38]

$$1 + z_{rec} = (1 + z_{Cosm})(1 + z_{Boost}), \quad (100)$$

where  $z_{Cosm}$  is the cosmological redshift due to the accelerated expansion of the Universe and  $z_{Boost}$  is a special relativistic redshift due to the peculiar motion produced by the local gravity effects (see [15–18] when the

geometry of the central objects was described by the Schwarzschild line element). In this relation, since  $z_{Cosm}$  and  $z_{Boost}$  do not depend on the metric, the cosmological redshift and the peculiar redshift become degenerate and we can just obtain  $z_{rec}$ , but not  $z_{Cosm}$  and  $z_{Boost}$  separately. On the contrary, since the dependency of  $z_{Cosm}$  on the metric derived in (91) as  $z_{Cosm} = H_0 r_d$  is explicit [or more completely in Eqs. (77)-(78)], this fact can help to break the degeneracy between  $z_{Cosm}$  and  $z_{Boost}$ , allowing us to estimate both of these frequency shifts separately.

As the final point, we would like to discuss how to measure the black hole parameters by employing this formalism a little bit. In order to apply the present method to real astrophysical systems, like the megamasers orbiting a central black hole in AGNs, one can use the approximation  $r_e \approx \delta r_d$  such that  $\delta$  is the aperture angle of the telescope that is a measurable quantity. Thus, in the case of static Schwarzschild black holes, the total redshift is a function of  $z_{Schw_{1,2}} = z_{Schw_{1,2}}(M, r_d)$  and we can employ Eq. (97) to compute the mass-to-distance ratio  $M/r_d$  in terms of the observable quantities  $z_{Schw_1}$  and  $z_{Schw_2}$ , as it was accomplished for the central black hole of NGC 4258 in [15] and more sixteen galaxies in [16–18]. Moreover, if the distance to the central black hole of the galaxy  $r_d$  is known from a different astrophysical experiment, then we can determine the Schwarzschild black hole mass  $M$  alone (see [16] for the TXS 2226-184 galaxy, for instance).

Alternatively, the total redshift is a function of  $z_{SdS_{1,2}} = z_{SdS_{1,2}}(M, r_d, \Lambda)$  in the case of SdS black holes, hence one can basically estimate  $M$ ,  $r_d$ , and  $\Lambda$  (or  $H_0$ ) with the aid of a statistical fit for AGNs within the Hubble flow. In this case, the Bayesian fitting method allows us to estimate  $M$ ,  $r_d$ , and  $\Lambda$  separately (not the mass-to-distance ratio  $M/r_d$ ) since the functional dependence of the total redshift on  $r_d$  in Eqs. (91)-(92) is different in the first term and the second term. With observational data detected from areas close enough to the black hole at hand, in principle we can also try to estimate the rotation parameter  $a$  by employing Eqs. (85)-(87).

#### IV. DISCUSSION AND FINAL REMARKS

In this paper, we have taken into account the KdS solutions and analytically obtained valid parameter space for having KdS black holes. Then, we have expressed the frequency shift of photons emitted by massive geodesic particles, stars for instance, that are circularly orbiting the KdS black holes in terms of the parameters of spacetime, such as the black hole mass, angular momentum, and cosmological constant. For this purpose, we have considered the detectors to be in radial motion with respect to the emitter-black hole system and employed a general relativistic formalism that was briefly described through the text.

In addition, we have seen that the shift in frequency

of photons increases with an increase in the cosmological constant as well as the detector distance to the emitter-black hole system that was compatible with the repulsive nature of the cosmological constant. Hence, this observation led us to extract the Hubble law from the original redshift formulas by taking into account some physically motivated approximations.

Moreover, we have found analytic expressions for the Schwarzschild black hole mass and the Hubble constant in terms of the observational frequency shifts of massive particles orbiting circularly this static spherically symmetric black hole. Interestingly, we have also shown that the Hubble law arose naturally from the exact formula of the Hubble constant (96). The concise and elegant formulas that we have found allow us to extract the properties of spacetime characterized by the black hole mass and spin as well as the cosmological constant through measuring shifts in the frequency of photons.

Now, we finish our paper with a couple of suggestions for future work. It would be interesting to employ and generalize this work in some other directions. For instance, in this study, we were interested in emitters in the range  $r_e \in [r_{ISCO}, r_{OSCO}]$  and far-away detectors within  $r_d \in (\bar{r}, r_c)$ , describing the black hole systems in the Hubble flow. However, this formalism can be generalized for circularly orbiting (or static) detectors as well for possible local tests of the accelerated expansion of the Universe. On the other hand, the formula (91) can be employed to estimate the Schwarzschild black hole mass  $M$ , the distance  $r_d$  to the black hole, and the Hubble constant  $H_0$  (or the cosmological constant  $\Lambda$ ) by using accretion discs circularly orbiting supermassive black holes hosted at the core of AGNs with the help of Bayesian fitting methods. Our primary estimations of  $H_0$  based on the observational data of galaxies within the Hubble flow show that this approach could be a powerful tool to obtain the Hubble constant alongside the black hole parameters. This investigation is currently under consideration.

Finally, we would like to stress that the  $H_0$  expression, that we obtained in (96) with the help of the KdS metric, represents a first step towards a more realistic parametrization of  $H_0$  in terms of observable quantities that also considers the matter content of the Universe, in consistency with the  $\Lambda$ -cold dark matter cosmological standard model. We are currently studying this problem and hope to report on it in the near future.

#### Acknowledgments

All authors are grateful to CONACYT for support under Grant No. CF-MG-2558591; M.M. also acknowledges CONACYT for providing financial assistance through the postdoctoral Grant No. 31155. A.H.-A. and U.N. thank SNI and PROMEP-SEP and were supported by Grants VIEP-BUAP No. 122 and No. CIC-UMSNH, respectively. U.N. also acknowledges support under Grant No. CF-140630.

- 
- [1] B. P. Abbott *et al.* (LIGO Scientific and Virgo Collaborations), *Phys. Rev. Lett.* 116, 061102 (2016).
- [2] K. Akiyama *et al.* (Event Horizon Telescope Collaboration), *Astrophys. J. Lett.* 875, L4 (2019).
- [3] K. Akiyama *et al.* (Event Horizon Telescope Collaboration), *Astrophys. J. Lett.* 930, L17 (2022).
- [4] A. Herrera-Aguilar and U. Nucamendi, *Phys. Rev. D* 92, 045024 (2015).
- [5] P. Banerjee, A. Herrera-Aguilar, M. Momennia and U. Nucamendi, *Phys. Rev. D* 105, 124037 (2022).
- [6] M. Sharif and S. Iftikhar, *Eur. Phys. J. C* 76, 404 (2016).
- [7] G. V. Kraniotis, *Eur. Phys. J. C* 81, 147 (2021).
- [8] D. Ujjal, *Chin. J. Phys.* 70, 213 (2021).
- [9] R. Becerril, S. Valdez-Alvarado, U. Nucamendi, P. Sheoran and J. M. Davila, *Phys. Rev. D* 103, 084054 (2021).
- [10] R. Becerril, S. Valdez-Alvarado and U. Nucamendi, *Phys. Rev. D* 94, 124024 (2016).
- [11] P. Sheoran, A. Herrera-Aguilar and U. Nucamendi, *Phys. Rev. D* 97, 124049 (2018).
- [12] L. A. Lopez and J. C. Olvera, *Eur. Phys. J. Plus* 136, 64 (2021).
- [13] L. A. Lopez and N. Breton, *Astrophys. Space Sci.* 366, 55 (2021).
- [14] Q. M. Fu and X. Zhang, *Phys. Rev. D* 107, 064019 (2023).
- [15] U. Nucamendi, A. Herrera-Aguilar, R. Lizardo-Castro and O. Lopez-Cruz, *Astrophys. J. Lett.* 917, L14 (2021).
- [16] A. Villalobos-Ramirez, O. Gallardo-Rivera, A. Herrera-Aguilar and U. Nucamendi, *Astron. Astrophys.* 662, L9 (2022).
- [17] D. Villaraos, A. Herrera-Aguilar, U. Nucamendi, G. Gonzalez-Juarez and R. Lizardo-Castro, *MNRAS* 517, 4213 (2022).
- [18] A. Villalobos-Ramirez, A. Gonzalez-Juarez, M. Momennia and A. Herrera-Aguilar, [arXiv:2211.06486].
- [19] S. M. Carroll, W. H. Press and E. L. Turner, *Annu. Rev. Astron. Astrophys.* 30, 499 (1992).
- [20] S. M. Carroll, *Living Rev. Rel.* 4, 1 (2001).
- [21] G. W. Gibbons and S. W. Hawking, *Phys. Rev. D* 15, 2738 (1977).
- [22] Z. Stuchlik and P. Slany, *Phys. Rev. D* 69, 064001 (2004).
- [23] E. Hackmann, C. Lammerzahl, V. Kagramanova and J. Kunz, *Phys. Rev. D* 81, 044020 (2010).
- [24] G. V. Kraniotis, *Class. Quantum Grav.* 28, 085021 (2011).
- [25] M. J. Reid, J. A. Braatz, J. J. Condon, L. J. Greenhill, C. Henkel and K. Y. Lo, *Astrophys. J.* 695, 287 (2009).
- [26] C. Y. Kuo, J. A. Braatz, J. J. Condon, C. M. V. Impellizzeri, K. Y. Lo, I. Zaw, M. Schenker, C. Henkel, M. J. Reid and J. E. Greene, *Astrophys. J.* 727, 20 (2011).
- [27] C. Y. Kuo, J. A. Braatz, M. J. Reid, K. Y. Lo, J. J. Condon, C. M. V. Impellizzeri and C. Henkel, *Astrophys. J.* 767, 155 (2013).
- [28] C. Y. Kuo, J. A. Braatz, K. Y. Lo, M. J. Reid, S. H. Suyu, D. W. Pesce, J. J. Condon, C. Henkel and C. M. V. Impellizzeri, *Astrophys. J.* 800, 26 (2015).
- [29] F. Gao, J. A. Braatz, M. J. Reid, K. Y. Lo, J. J. Condon, C. Henkel, C. Y. Kuo, C. M. V. Impellizzeri, D. W. Pesce and W. Zhao, *Astrophys. J.* 817, 128 (2016).
- [30] F. Gao, J. A. Braatz, M. J. Reid, J. J. Condon, J. E. Greene, C. Henkel, C. M. V. Impellizzeri, K. Y. Lo, C. Y. Kuo and D. W. Pesce, *Astrophys. J.* 834, 52 (2017).
- [31] D. W. Pesce, J. A. Braatz, M. J. Reid, J. J. Condon, F. Gao, C. Henkel, C. Y. Kuo, K. Y. Lo and W. Zhao, *Astrophys. J.* 890, 118 (2020).
- [32] C. Y. Kuo, J. A. Braatz, C. M. V. Impellizzeri, F. Gao, D. Pesce, M. J. Reid, J. Condon, F. Kamali, C. Henkel and J. E. Greene, *MNRAS* 498, 1609 (2020).
- [33] D. W. Pesce, J. A. Braatz, M. J. Reid, A. G. Riess, D. Scolnic, J. J. Condon, F. Gao, C. Henkel, C. M. V. Impellizzeri, C. Y. Kuo and K. Y. Lo, *Astrophys. J. Lett.* 891, L1 (2020).
- [34] B. Carter, *Phys. Rev.* 174, 1559 (1968).
- [35] J. M. Bardeen and J. A. Petterson, *Astrophys. J. Lett.* 195, L65 (1975).
- [36] J. Darling, *Astrophys. J.* 100, 837 (2017).
- [37] It does not matter whether the particle is co-rotating or counter-rotating due to the absence of the dragging effect produced by the rotation nature of spacetime. For more details see Fig. 3 of [5] and the related discussion.
- [38] T. M. Davis and M. I. Scrimgeour, *MNRAS* 442, 1117 (2014).